PHILOSOPHICAL TRANSACTIONS OF THE ROYAL SOCIETY A

Phil. Trans. R. Soc. A (2007) **365**, 3061–3084
doi:10.1098/rsta.2007.0020
Published online 14 September 2007

Chaotic stirring in quasi-turbulent flows

By Francois Lekien[1,*] and Chad Coulliette[2]

[1]*Université Libre de Bruxelles, Brussels 1050, Belgium*
[2]*California Institute of Technology, Pasadena, CA 91125, USA*

Transport in laminar flows is governed by chaotic stirring and striation in long thin filaments. In turbulent flows, isotropic mixing dominates and tracers behave like stochastic variables. In this paper, we investigate the quasi-turbulent, intermediate regime where both chaotic stirring and turbulent mixing coexist. In these flows, the most common in nature, aperiodic Lagrangian coherent structures (LCSs) delineate particle transport and chaotic stirring. We review the recent developments in LCS theory and apply these techniques to measured surface currents in Monterey Bay, California. In the bay, LCSs can be used to optimize the release of drifting buoys or to minimize the impact of a coastal pollution source.

Keywords: Lagrangian coherent structures; dynamical systems; chaos

1. Introduction

In all the branches of mechanical sciences, the concept of 'velocity' plays a central role. For example, Navier–Stokes equations describe how the velocity in a fluid changes with time. But is a fluid problem really solved when we know the velocity everywhere and at any given time?

Velocity and speed are abstract concepts that are not perceptible. While we can measure distance and time, we cannot measure speed directly. All 'velocity sensors' necessarily assimilate velocity with one of its effect. For instance, we evaluate the velocity of an oil spill by measuring the distance it travels in a given interval of time.

Not only is velocity difficult to measure, but also is a concept that neither a scientist nor an engineer can use directly. A driver is much more interested in knowing how much time it takes to travel a given distance rather than the speed of a vehicle. Coastguards are unconcerned with the velocity of an oil spill; instead, what they need to know is where the spill will be in a few hours and how its shape will deform. Likewise, when we are searching for a drifting boat on the ocean, the currents or the instantaneous velocity of the boat does not help in the recovery mission. What is needed is a prediction of the path followed by the drifting boat, and not its velocity.

In contrast to the classical Eulerian analysis of velocities, there is therefore room for a Lagrangian point of view where interest in trajectories dominates. At first, it seems that particle paths may be only a by-product of the velocity field.

* Author for correspondence (lekien@ulb.ac.be).

One contribution of 20 to a Triennial Issue 'Chemistry and engineering'.

Indeed, if we know the velocity $\boldsymbol{v}(\boldsymbol{x}, t)$ at any point $\boldsymbol{x}$, and at any time t, we can always compute the trajectory of a particle starting at the initial point $\boldsymbol{x}_0$ at time t_0 using

$$\boldsymbol{x}(t; t_0, \boldsymbol{x}_0) = \boldsymbol{x}_0 + \int_{t_0}^{t} \boldsymbol{v}(\boldsymbol{x}(\tau; t_0, \boldsymbol{x}_0), \tau)\mathrm{d}\tau,$$

where the notation $\boldsymbol{x}(t; t_0, \boldsymbol{x}_0)$ indicates that the trajectory is a function of time t, but also depends on the initial position $\boldsymbol{x}_0$ and the initial time t_0. Among all the solutions, $\boldsymbol{x}(t; t_0, \boldsymbol{x}_0)$ is the one satisfying $\boldsymbol{x}(t_0) = \boldsymbol{x}_0$. The equation above shows that the particle trajectory is the solution of a Volterra integral equation of the second kind (Arfken 1985, p. 865). Provided that the velocity is smooth enough, one can always compute a unique trajectory through any initial condition. Furthermore, a vast amount of algorithms are available to compute the trajectories numerically (Cellier & Kofman 2006).

This perspective seems to corroborate the fact that the Lagrangian description of transport in a fluid can always be derived from the velocity. It prevailed until the discovery of dynamical chaos in the early 1960s. Lorenz (1963) found out that a slight error in the initial condition $\boldsymbol{x}_0$ could lead to dramatic errors in the position at a later time $\boldsymbol{x}(t)$. This 'butterfly effect' was later detected in a vast amount of physical systems: sensitivity to initial conditions is the rule and not the exception.

Owing to the finite resolution of sensors, we cannot measure the initial position $\boldsymbol{x}_0$ perfectly, and dynamical chaos interferes with our knowledge of the world. Even if the velocity field $\boldsymbol{v}(\boldsymbol{x}, t)$ was known perfectly everywhere and at all times, it would still be impossible to predict, even approximately, the path of a particle for an infinite time (Stewart 1989). Indeed, the uncertainty on the position grows exponentially and eventually becomes prohibitive.

Another consequence of dynamical chaos is the complexity of the trajectories, which must eventually diverge and separate. Provided that we integrate the particles for long enough, each trajectory is unique and cannot resemble its neighbours. The Lagrangian description of the fluid is therefore very complex and one would need to compute and analyse millions of trajectories to characterize all the possible behaviours present in the system.

Dynamical systems theory aims at finding transport barriers and a geometric description of transport in the complexity of the trajectories. It provides a few coherent structures from which the general behaviour of particles can be deduced.

Advanced textbooks (Guckenheimer & Holmes 1983) give us recipes for determining transport barriers in steady systems. This procedure can be generalized to time-periodic systems (Smale 1980; Rom-Kedar 1990) and is summarized in §3. Outside the steady and periodic *laminar* regimes, the dynamical systems analysis requires a careful investigation of the relative importance of stirring and mixing (see §2) and a generalization of the concept of coherent structures, which we investigate in §§3 and 4.

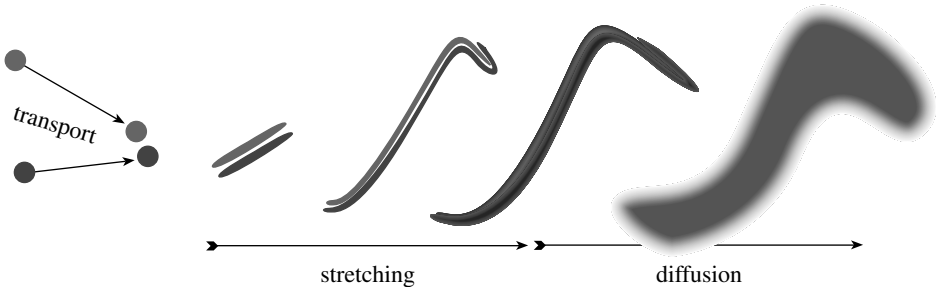

Figure 1. Stirring (transport and stretching) followed by diffusive mixing. Macroscopic patches of dye are stirred by a velocity field: fluids with different dye colours are transported over long distances, stretched and brought in close contact. Once chaotic stirring has stretched the tracers on sufficiently small length scales, diffusion takes over and mixes the dye irreversibly.

2. Stirred, then mixed

(*a*) *Advection and diffusion*

The evolution of a passive tracer $c(\boldsymbol{x}, t)$ (e.g. dye, temperature, concentration of spilled oil) in continuous media where the velocity field is $\boldsymbol{v}(\boldsymbol{x}, t)$ is governed by the advection–diffusion equation

$$\frac{\mathrm{D}c}{\mathrm{D}t} = \frac{\partial c}{\partial t} + \underbrace{\boldsymbol{v}\cdot\nabla c}_{\text{advection: } UC/l} = \underbrace{\kappa\nabla^2 c}_{\text{diffusion: } \kappa C/l^2} + \underbrace{J_c}_{\text{source}},$$

where κ is the molecular diffusivity and $J_c(\boldsymbol{x}, t)$ is the (possible) source of the tracer (forcing). The advection term represents the stirring of the tracer by the velocity field $\boldsymbol{v}$. It is a reversible process where fluid elements are transported across the domain, rotated, stretched and folded (figure 1). Even for very simple velocity fields, the combined action of stretching and folding of fluid elements generates complex patterns, hence the name 'chaotic advection' or 'stirring'.

The diffusive term generates irreversible mixing of the tracer. In the absence of a source J_c, this term homogenizes the distribution of the tracer at an exponential rate and blurs the structures present in the initial distribution as well as the patterns created by chaotic stirring (see last step in figure 1).

Chaotic stirring and turbulent mixing are competing processes and it is critical to evaluate their relative importance (Ottino 1999). If U and C denote a characteristic velocity and a typical tracer concentration, and if the tracer varies over length scales l, the stirring term is of the order UC/l. On the contrary, the diffusive term behaves as $\kappa C/l^2$. The relative importance between stirring and diffusion can therefore be approximated by

$$Pe(l) = \frac{U(l)l}{\kappa}.$$

Both $U(l)$ and $Pe(l)$ vary considerably depending on the wavelength l of the tracer. At the scales of the fluid domain, the ratio Pe corresponds to the Péclet number and is almost always large except for extremely small-scale phenomena with low velocities (Haynes 2003).

This does not, however, imply that diffusion is always negligible. For instance, we all know that milk and coffee can be quickly mixed in a cup. The key to understanding the subtle interaction between stirring and mixing is to

realize that their relative importance is a function of the tracer length scale l. For small length scales, both $U(l)$ and l are small and diffusion is more important. From an initial macroscopic patch of tracer, or in a macroscopically forced tracer, the advective term is, initially, the absolute ruler of the fate of the tracer (i.e. large $Pe(l)$ for large l). Nevertheless, the advective term stretches and folds parcels of fluid (figure 1). Two fluid elements containing different tracer concentrations are stretched into long filaments which the velocity field brings together at exponential rates, creating higher gradients. The initially dominant advective term decreases the length scale of the tracer variations and, as a result, increases the influence of the diffusive term. In highly stretched regions, or *hyperbolic areas*, the length scale of the tracer becomes so small that $Pe(l)$ drops below unity and isotropic diffusion is the only process acting on the tracer distribution.

Dropping milk (i.e. the tracer) in a cup of coffee (i.e. the fluid) exhibits all the aspects of the process described above. An initial macroscopic parcel of milk at the surface of the coffee does not mix quickly on its own. At the length scale of the cup, Pe does not allow any mixing. A spoon is an effective tool to get the advection–diffusion machine in action. By stirring the coffee, we generate a velocity field $\boldsymbol{v}$ on the surface. The advection creates long filaments of milk and brings them close to areas where coffee is still pure. In these regions, the gradient is high; on such small length scales, Pe favours diffusion and milk can finally mix, irreversibly, with the coffee. We can also observe the direct effect of the molecular diffusivity κ: cold coffee (smaller κ) requires more stirring since, at the same length scale l, the ratio Pe is higher.

Note that, in this paper, we do not consider the effect of the source J_c on the tracer distribution. Indeed, we aim at understanding the evolution of an oil spill, the fate of drifting buoys or the impact of contaminants. In these cases, the tracer is released at a specific time (initial condition) and the source term J_c is unused. In most cases, external injection of tracer in the system does not modify the framework presented in this paper. Indeed, injection or forcing at the macroscopic length scales follows the same length-scale reduction process described in figure 1. The situation is, however, different if the source also acts on microscopic length scales (e.g. chemical or biological activity). In this case, the presence of microscopic sources and sinks alters the tracer dynamics and modifies the coherent structures (Giona *et al.* 2002; Tél *et al.* 2005).

As shown in figure 1, in the absence of microscopic sources, there are two distinct steps in the evolution of a tracer. First, from a reference length scale L, chaotic stirring stretches the fluid elements containing the tracer in thin filaments. The duration of that process can be determined by following a reference trajectory $\boldsymbol{x}(t)$ and a nearby particle $\boldsymbol{x}(t)+\boldsymbol{\delta}(t)$. Since diffusion is negligible during the first stage, the difference between the two particles follows

$$\frac{\mathrm{d}\boldsymbol{\delta}}{\mathrm{d}t} = \underbrace{\frac{\partial \boldsymbol{v}}{\partial \boldsymbol{x}}}_{\text{velocity gradient}} \boldsymbol{\delta}.$$

The fast reduction of length scale, or hyperbolic stretching, is possible due to large negative eigenvalues in the velocity gradient. The magnitude of the velocity gradient determines how fast advection can shrink the length scale of the tracer down to the diffusive length scale.

(*b*) *Laminar, quasi-turbulent and turbulent regimes*

To understand the evolution of a tracer in continuous media, it is therefore critical to investigate the velocity field $\boldsymbol{v}$ and determine the distribution of the velocity gradient. Navier–Stokes equations reveal that the evolution of the velocity field is governed by a balance between a convective term, a viscous term and external forcing. The Reynolds number Re is the ratio between the magnitude of the convective and viscous terms. At low Reynolds numbers, the viscous forces are high and energy input from the forcing is dissipated easily; if a feature with a very small length scale is created, it is immediately dissipated by the large viscous forces. Such a laminar flow has large, simple structures, and, from the point of view of a scalar tracer, transport is typically delineated by steady or periodic stretching structures.

On the contrary, a large Reynolds number indicates that viscous forces are not important at the flow scale. The solution contains eddies with a broad range of diameters. The smallest length scale contained in the velocity field $\boldsymbol{v}$ is referred to as the Kolmogorov microscale l_ν. The kinetic energy in the flow cascades from the macroscopic scale down to l_ν under the dynamics of smaller and smaller eddies.

Kolmogorov (1941) showed that the difference between the macroscopic length scale and the Kolmogorov length scale is given by the Reynolds number.[1] When the Reynolds number is very large, the Kolmogorov scale becomes comparable to the diffusion length scale. This is the turbulent limit where chaotic advection is non-existent since tiny eddies immediately deform the tracer concentration on length scales where diffusion takes place. Turbulent flows are characterized by immediate diffusion. In such flows, studying advection is irrelevant; statistical methods are more appropriate tools for studying isotropic turbulence.

But nature is far from being made exclusively of laminar, advective flows and turbulent, stochastic flows. Most natural fluids and geophysical flows correspond to an intermediate situation: the quasi-turbulent regime. In this case, the Reynolds number is high and l_ν is small, but still much larger than the diffusion length scale. In such flows, there is a phase of chaotic advection where fluid elements are stretched, followed by a diffusion stage (figure 1). In such flows, stochastic methods alone cannot explain the distribution of a tracer; one needs to understand how the advection of the velocity field delineates particle trajectories before diffusion takes place.

Can we ignore the small-scale features during the advection stage? Can we approximate a quasi-turbulent flow with only its largest features and apply the classical dynamical systems tools to study advection? Unfortunately, as shown by Haynes (2003), and as we will verify in §5, the most significant stretching does not usually occur at the largest macroscopic length scales, but at the smallest length scale l_ν. At best, stretching is equally distributed among all the length scales of the quasi-turbulent fluid. This is precisely what makes this problem so challenging: transport, coherent structures and stretching in a quasi-turbulent fluid involve a broad range of time scales and length scales, from the macroscopic length scale where the velocity is high and the velocity gradient is small, down to the Kolmogorov length scale, where the velocity is small and the velocity gradient is high (Rom-Kedar & Poje 1999).

Another challenge of the quasi-turbulent regime is the finite-time nature of the observed structures. At low Reynolds numbers, the flows exhibit steady, periodic or quasi-periodic structures. The resulting coherent structures (eddies, transport

[1] Hinze (1975) showed that the ratio between the largest and smallest length scales is given by $Re^{3/4}$.

barriers, convection cells) last forever and are easily identified by classical dynamical systems analysis. On the contrary, quasi-turbulent flows have a much more complex time dependence. Not only do we find large velocity gradients on a broad range of small time scales but also the large-scale features will vary and wander between different regimes. One such example is the Antarctic ozone hole. While the dynamics of ozone is well captured by a single vortex oscillating near the South Pole, this structure splits regularly into smaller eddies (Varotsos 2002). Similarly, large anticyclonic rings detach regularly from the Gulf Stream. These rings live for approximately 1 year during which they organize waters and tracers in coherent gyres. None of these structures can be understood nor detected by classical dynamical systems theory, which is based on the asymptotic (i.e. infinite time) behaviours of particles. In the quasi-turbulent regime, coherent structures may live and act only for a finite period of time. Not only do we need to adapt to an aperiodic time dependence but also the theory must allow for impermanent and changing coherent structures (Haller & Poje 1998; Poje & Haller 1999). The notions of fixed points, invariant manifolds, exponential stretching and chaotic dynamics must be understood in the context of systems that are known or studied only for a finite-time window (Haller 2000).

3. Stirred, but not mixed

Classical dynamical systems theory provides an adequate framework for transport in laminar flows: the large-scale features dominate and give rise to Lagrangian coherent structures (LCSs), such as KAM tori, and the invariant manifolds of hyperbolic fixed points or periodic orbits. The LCSs divide the phase space into regions of qualitatively different dynamics (e.g. jets, eddies, gyres, alleyways).

In this section, we summarize and illustrate classical dynamical systems theory for laminar (steady, periodic and quasi-periodic) flows. Next, we investigate how these methods extend to the quasi-turbulent regime where many different length scales and time scales coexist. In such flows, 'moving' LCSs continue to separate the flow into regions of qualitatively different dynamics and their entanglement generates chaotic stirring.

(*a*) *Steady regime*

Figure 2 illustrates the dynamical systems framework for a steady flow. The flow corresponds to the stream function $\psi = A\sin(2x)\sin(2y)$ and is a rough dynamical approximation of the flow after the first instability in Rayleigh–Bénard convection cells (Solomon & Gollub 1988). The fluid is heated on the lower boundary ($y=0$) and propagates upwards along $x=\pi/2$. When it reaches the cold boundary at the top ($y=\pi/2$), the stream separates before it returns to the lower boundary. As shown in figure 2, for a steady flow, Eulerian and Lagrangian descriptions are equivalent: the Lagrangian streamlines in figure 2*b* can be easily deduced from the Eulerian velocity vectors of figure 2*a*.

Two points in the flow are highly distinguished. On the bottom boundary, the point $(x, y)=(\pi/2, 0)$ has zero velocity (fixed point) and corresponds to the collision between the two streams propagating in opposite directions along the lower boundary. On the top boundary, the point $(x, y)=(\pi/2, \pi/2)$ is also a

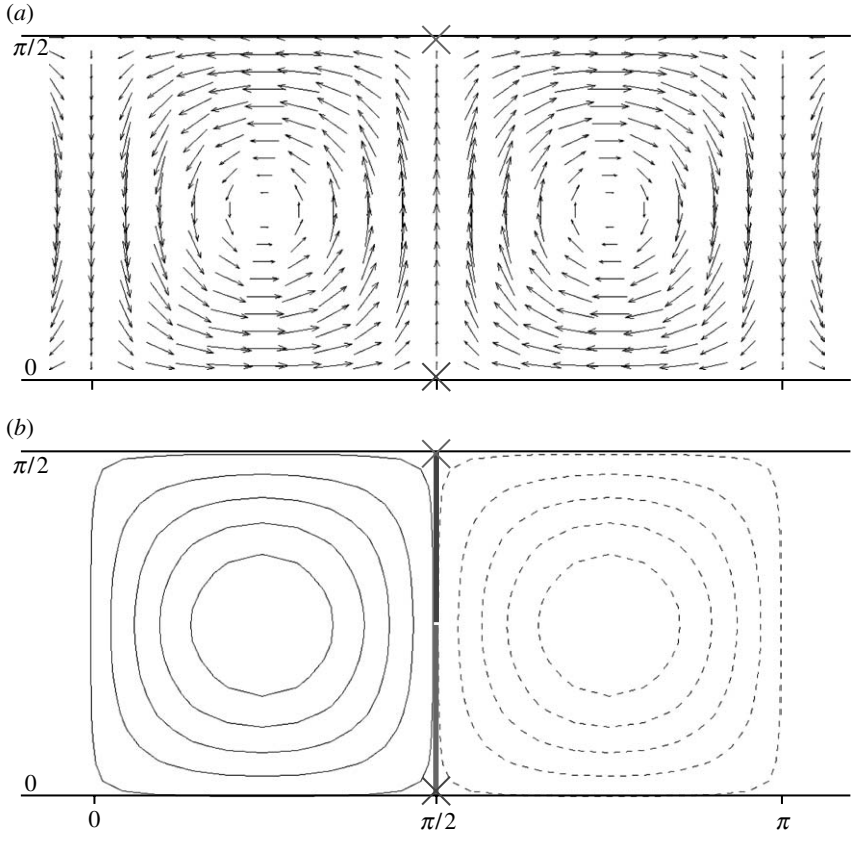

Figure 2. Transport in a steady flow. There is an invariant manifold (thick line) connecting the two saddle points (crosses) on the boundary and preventing any transport between cells. (*a*) Velocity vectors and (*b*) streamlines $\psi = A\sin(2x)\sin(2y)$. Solid lines correspond to anticlockwise motion and dashed lines to clockwise rotation.

fixed point and it marks the separation of the fluid into two streams travelling in opposite directions. These points are called *hyperbolic* fixed points since, in their vicinity, both stretching and shrinking coexist.

The two points have hyperbolic stable and unstable manifolds. The stable manifold of the fixed point $(x, y) = (\pi/2, \pi/2)$ is the set of points that converge to the fixed point. The unstable invariant manifold of the fixed point $(x, y) = (\pi/2, 0)$ is the set of points that converge to the fixed point in backward time. As shown in figure 2*a*, these two invariant manifolds are identical and delineate a vertical LCS that divides the domain into regions of qualitatively different dynamics. In this case, the LCS marks the boundary between the anticlockwise cell on the left and the clockwise cell on the right. It also determines transport between these regions. In this case, and for all two-dimensional steady flows, there is no fluid exchange between the cells; the LCS forms an uncrossable barrier between the two cells rotating in opposite directions.

This construction leads to an important conclusion: there is never any chaos in a steady two-dimensional flow. Chaos can only occur if we add a third dimension or when the system is unsteady (see Poincaré–Bendixon theorem in Guckenheimer & Holmes (1983)).

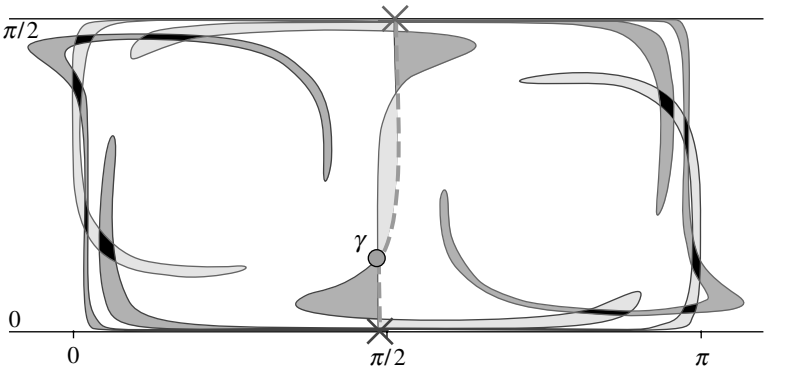

Figure 3. Hyperbolic invariant manifolds in a periodic system. The hyperbolic fixed points of the Poincaré map have a stable and an unstable invariant manifold (solid curves) intersecting in many lobes. A boundary (dashed line) between cells is constructed by picking one of the intersection points (γ) and joining segments of the two manifolds.

(*b*) *Periodic regime*

The convection cells of Solomon & Gollub (1988) can be made periodic by setting $\psi = A\sin(2(x - g(t)))\sin(2y)$ where $g(t)$ is a periodic function. This flow is identical to the steady case, except that the cell pattern is now oscillating periodically. There are still points where the velocity is instantaneously zero on the horizontal boundaries, but they are now moving. These critical points are no longer *fixed* and are called *stagnation points* (Coulliette & Wiggins 2001).

To build coherent structures similar to the barrier in the steady flow, we use the elegant theory of Poincaré maps (Poincaré 1890). For periodic systems, Poincaré's idea is to take 'snapshots' of the dynamics.[2] Instead of following particles continuously, he looks at the net displacement after a time step equal to the period of the oscillations. There are no fixed points in the continuous system, but Poincaré is interested only in points that return to their initial position after a time equal to the period of the oscillation.

The invariants of the Poincaré map are periodic trajectories. As shown in figure 3, there are two such hyperbolic trajectories located near the position of the saddles of the steady system. In periodic systems, however, the associated invariant manifolds do usually not overlap, they intersect and form sequences of lobes.

As described in Smale (1980) and Guckenheimer & Holmes (1983), to define a boundary between cells, it is convenient to pick one of the intersection points (this so-called boundary intersection point or 'bip' is indicated as a circle and marked γ in figure 3). The separatrix between the cells is constructed by joining a segment of unstable manifold (from the hyperbolic point on the lower boundary to the bip) to a segment of stable manifold (from the bip to the hyperbolic point on the top boundary).

Figure 4 investigates transport between the left and right cells in the periodic system. The efficiency of the dynamical systems framework stems from the fact that the lobes are mapped exactly onto themselves after a time equal to the

[2] Henri Poincaré developed his methods for the three-body problem in the late 1880s. It is conceivable that he came across chaos at that time, but the value of Poincaré maps for studying chaos in periodic systems was discovered by Stephen Smale only in 1965 (Smale 1980).

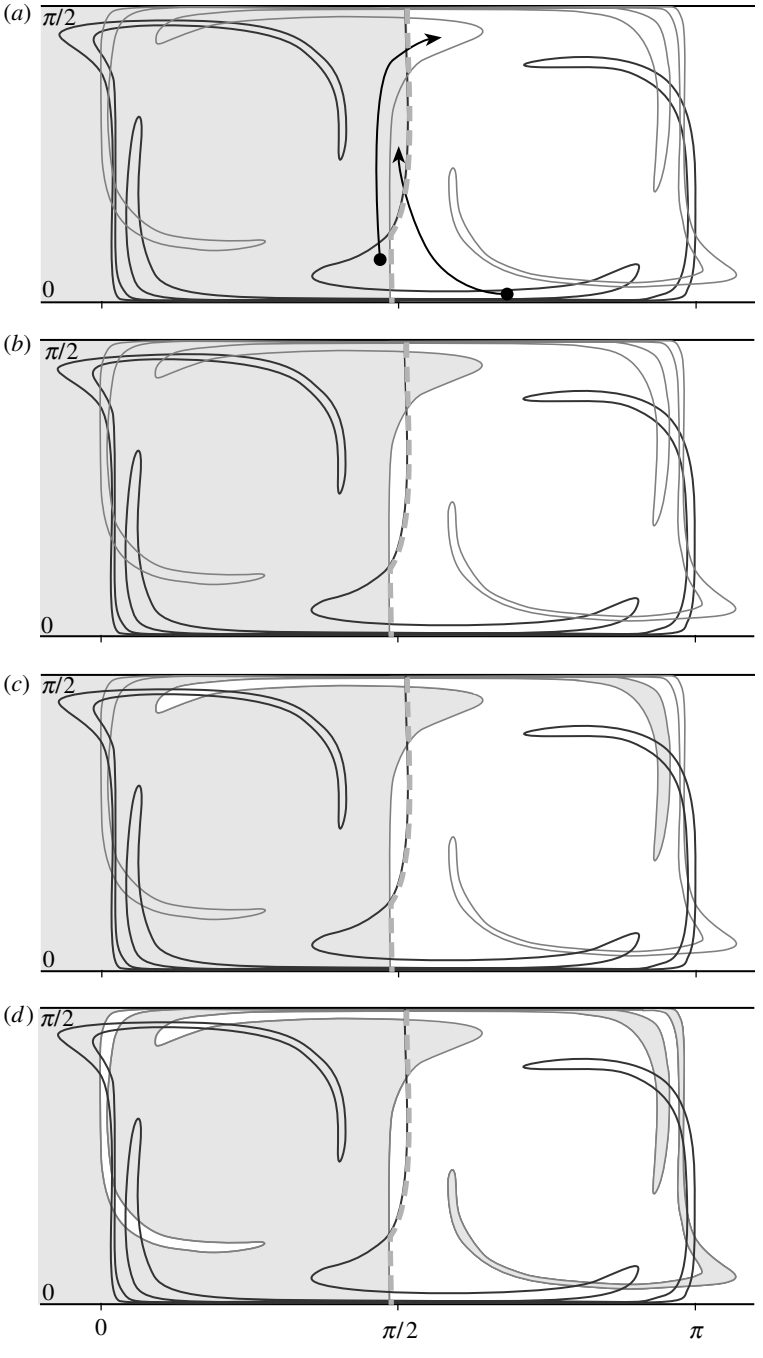

Figure 4. (*a–d*) Transport in a periodic system. Dark dye in the left cell penetrates the right cell as it fills the lobes between the LCSs. Each picture corresponds to a successive Poincaré mapping.

period of the system. In figure 4, we follow the drift of dark dye released in the left cell. The snapshots in figure 4 show that transport is governed by the lobes comprised between the coherent structures.

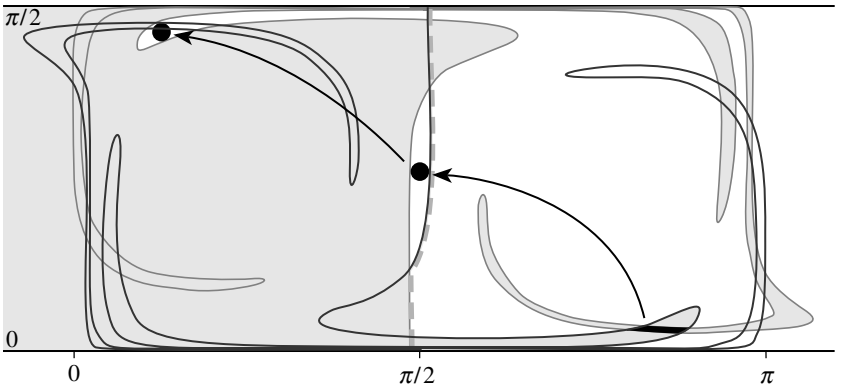

Figure 5. Lobe overlapping induces chaotic stirring.

How is chaos generated in the periodic system? A general construction, known as the Smale horseshoe, gives the paradigm for chaotic advection (Smale 1980; Guckenheimer & Holmes 1983). The key ingredient is the entanglement of the lobes. As shown in figure 5, the dyed lobes in the right cell (i.e. containing fluid that was entrained from the left cell) eventually intersect with the other sequence of lobes (i.e. fluid that will be detrained to the left cell). While our initial description of transport in terms of lobes only took into consideration single-step transport from one cell to the other, the intersections between lobes indicate more complex dynamics. In the intersection between the lobes, the particles must obey the dynamics dictated by each overlapping lobe.

Let us denote by 0 and 1 the position of a particle in the left and right cells, respectively. Using this 'symbolic dynamics', the history of a particle can be represented as a string of 0s and 1s. For example, a particle that crosses from left to right contains '…01…' in its string. The intersections between the lobes guarantee that all possible strings (or histories) are possible. No matter how complicated the desired sequence of 0 and 1 is, there is a particle in the system that corresponds to it. Moreover, no matter what the history is up to the present time, all future behaviours are possible (Guckenheimer & Holmes 1983).

Mathematically, the existence of chaotic dynamics in the system is proved by showing that there is a chaotic invariant Cantor set in the entanglement of the lobes. Smale's geometric construction is universal: as long as lobes intersect, there exists a fractal invariant set that is sensitive to initial conditions. The fractal dimension and the location of the chaotic invariant set (also called 'chaotic saddle') provide useful information about asymptotic mixing (see Tél *et al.* (2005) for a recent review). The chaotic fractal set has also its own stable and unstable limit sets, but these should not be confused with the stable and unstable manifolds studied in this paper. As we will show in §4, generalizing the definition of chaotic invariant sets to quasi-turbulent flows is difficult since the notion of invariance must be replaced by the concept of boundedness, which is not Galilean invariant. Instead of working directly on the chaotic set, we concentrate on generalizing coherent structures for quasi-periodic systems. Once coherent structures are properly defined and intersect in sequences of lobes, a construction similar to Smale (1980) gives the corresponding chaotic sets, this time without any violation of the Galilean invariance.

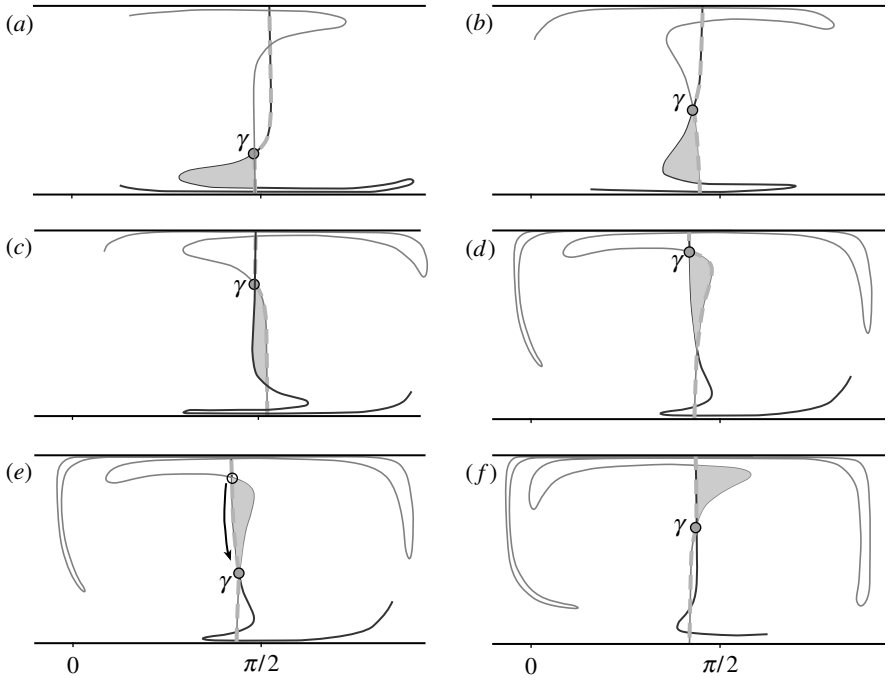

Figure 6. Lobe dynamics in an aperiodic system. A boundary intersection point (bip) between the invariant manifolds is selected and defines the cell interface (dashed line). (*a–d*) As time evolves, the bip moves up and the interface deforms to the point where it no longer describes an acceptable boundary. (*e*) At this time, the bip must be changed, which triggers the switch of lobes from one cell to another.

(*c*) *Quasi-turbulent regime*

For steady and periodic flows, stable and unstable invariant manifolds of hyperbolic fixed points and periodic orbits provide adequate LCSs. If the flow is not periodic but very close to periodic, a similar framework can be derived in second-order Poincaré maps (Parker & Chua 1989, ch. 2.3). But what can we do for general systems that are far from the laminar limit?

In a quasi-turbulent flow, the energy spectrum is broad: the velocity gradient is significant at all scales and it is never acceptable to restrict the flow to a few periodic oscillations, precluding the use of Poincaré maps. Nevertheless, LCSs continue to divide the flow into regions of qualitatively different dynamics and govern chaotic transport (Voth *et al.* 2002).

Defining and computing the LCSs for such flows is an active area of research which we discuss in §4. It is, however, worth taking a look at how intersecting lobes continue to generate chaotic transport in the aperiodic case. Figure 6 shows the LCSs in the aperiodic system. The stream function is still $\psi = A\sin(2(x-g(t)))\sin(2y)$, but this time the function $g(t)$ is replaced by an aperiodic function. To obtain a truly aperiodic (but smooth) function, we proceed as follows: we compute the Fourier spectrum of a sequence of uncorrelated random numbers and fit the amplitude of the spectrum to that of a random process with Gaussian covariance. The inverse Fourier

spectrum of the last spectrum gives us an aperiodic function $g(t)$ which is a smooth realization of a random process with prescribed covariance in time (see Lekien & Haller (in press) for a complete description).

As in the periodic case, a bip γ is selected to construct a boundary between the cells (figure 6). However, in this case, the bip, the boundary and the lobes evolve with time. In particular, the bip moves up towards the top boundary, and the boundary quickly becomes obsolete as the unstable manifold oscillates near the top boundary. At this time, the bip must be changed and a more acceptable boundary must be reconstructed. When the bip and the boundary change, some lobes will find themselves on the other side of the boundary.

This framework for transport in aperiodic systems was introduced by Coulliette & Wiggins (2001) and generalized the Smale horseshoe to quasi-turbulent systems: as long as we have intersecting lobes, chaotic stirring takes place. Furthermore, a (moving) chaotic set is found in the entanglement of the lobes (see §6 of Tél *et al.* (2005)). It is worth noting that the example of figure 6 was designed in such a way that the LCSs could be easily computed. While the time dependence is truly aperiodic, the general structure of the convection cell never changes and the analytic flow is known at all past and future times. In a more realistic flow, such everlasting LCSs do not exist, and it is usually not possible to find such everlasting hyperbolic trajectories on the boundary with unique stable and unstable manifolds. In §4, we investigate the definition of LCSs and take into account the finite-time nature of the structures.

4. Lagrangian coherent structures

As shown in the previous sections, advection in the laminar and quasi-turbulent regime is well described by LCSs. The LCSs divide the fluid into regions of qualitatively different dynamics; their entanglement and the resulting lobes govern chaotic transport between the regions.

In steady and periodic laminar systems, LCSs correspond to hyperbolic invariant manifolds of fixed points and periodic orbits (Guckenheimer & Holmes 1983); they are easily computed and fully govern transport. Indeed, it takes a considerable length of time for a laminar flow to stretch a tracer down to the diffusive length scale.

In quasi-turbulence, high velocity gradients at small scales trigger diffusion more rapidly. Nevertheless, the LCSs from the advective stage remain active for a significant time; even when diffusion takes place, the footprints of the LCSs survive as they created inhomogeneous stretching and the relative importance of diffusion varies depending on the position with respect to the LCSs. Furthermore, most geophysical flows are fuelled by large-scale external forces. The LCSs act constantly to stretch the incoming tracer. One such example is the Gulf Stream: the constant cooling in the sub-polar gyre and the constant warming in the subtropical gyre induce a sustained action of an LCS dividing those two gyres. The dynamics of particles and tracers is dominated by this everlasting LCS. Diffusion weakens the relevance of LCSs in quasi-turbulent flows but rarely blurs the advective patterns completely.

In this section, we investigate how to identify LCSs in quasi-turbulence. The broad range of length scales present in the quasi-turbulent regime makes it far from being steady or periodic. We need a new definition of LCS for aperiodic

flows. Furthermore, this definition has to accommodate finite-time LCSs, as well as their appearance and disappearance.

Three approaches to this problem can be found in the literature. First, one can seek strong, non-rotating, hyperbolic stagnation points that never bifurcate. Haller & Poje (1998) showed that, near such a point, there exists a hyperbolic trajectory and associated invariant manifolds. Sandstede *et al.* (2000) illustrated this method. Unfortunately, the strong hypothesis on the stagnation points is seldom satisfied for many flows of interest. Stagnation points often bifurcate or spin rapidly near a smaller scale eddy. Both processes violate the hypothesis of Haller & Poje (1998) and leave us no clue about the location, or even the existence, of an LCS.

A second approach was proposed by Ide *et al.* (2002). Even for stagnation points wandering over large areas, Ide *et al.* (2002) suggested linearizing the flow inside the box where the stagnation point moves and restricts the analysis to the Eulerian linearization of the flow inside the box. Unlike the full nonlinear flow, the linearized approximation induces the same stretching everywhere in the box and an infinite number of hyperbolic trajectories can be computed. To segregate the hyperbolic trajectories in the linear flow, Ide *et al.* (2002) showed that only one of the trajectories remains bounded in the linear approximation and elected it to the status of *distinguished hyperbolic trajectory*.

As shown by Mancho *et al.* (2004), the method can be very powerful and accurate in some flows. Its main weakness is the fact that it violates a fundamental law of physics: Galilean invariance. No matter how we define LCSs, one expects the definition to be invariant with respect to uniform translations of the coordinate frame. But neither the stagnation points nor the notion of boundedness is frame invariant. Following Ide *et al.* (2002), an observer standing on shore and an observer flying at constant speed in an aircraft may be observing the exact same flow and compute different *distinguished hyperbolic trajectories*.

Methods based on stagnation points were even more challenged recently when specific examples dissociating LCSs and hyperbolic stagnation points were discovered. Haller & Poje (1998) already noted that an LCS did not necessarily exist in the neighbourhood of a hyperbolic stagnation point. But the discovery of LCSs existing in the absence of any hyperbolic stagnation point discredited all the methods based on stagnation points (Lekien & Haller in press). The elegant theory of LCS for steady and periodic flows makes an intensive use of hyperbolic stagnation points and this misled us into overestimating their role in quasi-turbulent dynamics. In fact, stagnation points are important in steady and periodic flows only because, in such flows, they are also the *strongest hyperbolic trajectories*. In aperiodic flows, stagnation points are no longer trajectories and are, hence, irrelevant in describing transport, stretching and LCSs. Stagnation points are not Galilean invariant in quasi-turbulent flows; they disappear and appear depending on the speed of the coordinate frame and they cannot, therefore, participate in a coherent theory of stretching and LCSs that are intrinsic, Galilean invariant properties of the fluid dynamics.

For the same reason, the direct generalization of the chaotic Cantor set (i.e. the chaotic saddle delineated by the entangled LCSs) to quasi-turbulent flows is difficult. For fixed obstacles in open flows, it is sometimes possible to find a 'stagnant chaotic fractal set' (see §7 of Tél *et al.* (2005)). Nevertheless, this concept can hardly be applied to arbitrary flows. Notions such as 'stagnation' or

'boundedness' eventually violate Galilean invariance and lead to contradictions. Instead, we seek a Galilean invariant extension of smooth LCSs for quasi-periodic flows. The generalized chaotic sets then follow naturally from Smale's construction.

The concept of locally *strongest hyperbolic trajectory* received its first mathematical formalism in a seminal paper by Haller (2000) where the existence of attached LCSs is formally demonstrated. Later, Shadden *et al.* (2005) showed that the LCSs attached to the strongest hyperbolic trajectory were also very close to the strongest attractive and repulsive lines in the flow, connecting with the vast amount of dye experiments in fluid mechanics (Voth *et al.* 2002). The theory of the strongest hyperbolic trajectories and the concept of the most hyperbolic LCSs guarantee frame invariance. Furthermore, they no longer rely on the capricious meandering of stagnation points. Their application is limited only by the destructive effect of diffusion (an unavoidable limit) and aperiodic LCSs quickly conquered transport problems in various fields of engineering and science, from geophysical flows (Lermusiaux *et al.* 2006) to space travel (Ross 2006) and from algal blooms (Olascoaga *et al.* 2006) to underwater vehicle control (Bhatta *et al.* 2005).

The LCS theory can be seen as an attempt at avoiding the pitfalls of the other methods and as a retreat behind a more primitive concept: the deformation tensor. If we consider a trajectory $\boldsymbol{x}(t)$, an infinitesimal perturbation about its initial condition evolves as $\boldsymbol{\delta}(t) = X(t;\, t_0,\, \boldsymbol{x}_0)\boldsymbol{\delta}_0$, where $X(t;\, t_0,\, \boldsymbol{x}_0)$ is the fundamental solution matrix or the finite (linear) deformation tensor. The advantage of this approach is that Galilean invariance is inherited from the properties of the deformation tensor. Also, it does not require any assumptions about the velocity field or its stagnation points since finite deformations (and not infinitesimal changes due to the instantaneous velocity field) are playing a central role. From the Volterra equation mentioned in §1, one can derive the deformation tensor as

$$X(t;\, t_0, \boldsymbol{x}_0) = \frac{\partial \boldsymbol{x}(t;\, t_0, \boldsymbol{x}_0)}{\partial \boldsymbol{x}_0},$$

i.e. the matrix which gives the change in final position $\boldsymbol{x}(t;\, t_0,\, \boldsymbol{x}_0)$ due to an infinitesimal change in the initial condition $\boldsymbol{x}_0$. In the absence of the elegant simplifications arising in steady and periodic flows, the aperiodic LCS theory returns to its more primitive, but seminal, concept: sensitivity to initial conditions.

It is worth mentioning that the LCS theory is far from being complete and frozen. To compute the finite-time deformation tensor $X(t;\, t_0;\, \boldsymbol{x}_0)$, several choices are possible. Haller (2000) and Shadden *et al.* (2005) used a fixed horizon and approximated $X(t;\, t_0;\, \boldsymbol{x}_0)$ by numerically differentiating a grid of a particle integrated for a constant time. But Koh & Legras (2002) showed that fixing the size of the initial and final perturbations and computing the time it takes to go from one to another can give a more pronounced approximation of the deformation tensor in some cases. It is also possible to identify a fixed time window and restrict the computation of the Lyapunov exponent to a specific time interval. Such a procedure is particularly interesting when the flow can be divided, *a priori*, into distinct regimes (Lekien & Leonard 2004).

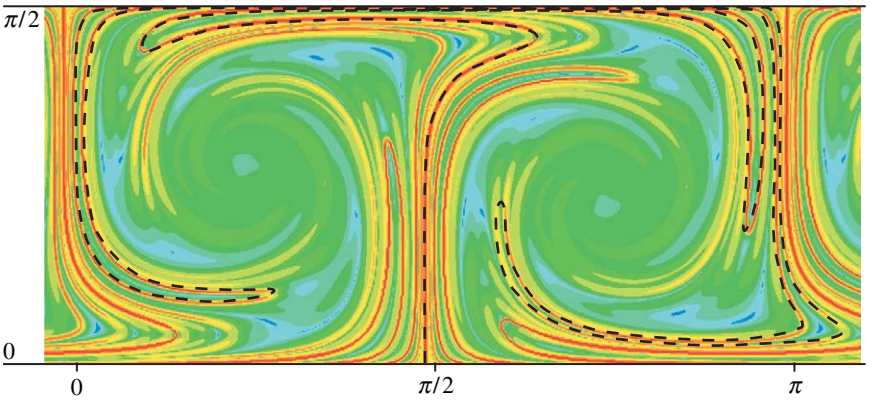

Figure 7. Finite-time Lyapunov exponent and LCS. Red denotes high stretching and blue corresponds to areas that will not be stretched. The LCS are ridges (dashed line) in the Lyapunov exponent landscape.

Furthermore, the stretching indicator used today is based on the polar decomposition of the deformation tensor. The maximum singular value of X,

$$\sigma = \max_{\boldsymbol{\delta}} \frac{\|X\boldsymbol{\delta}\|^2}{\|\boldsymbol{\delta}\|^2},$$

is used to approximate the stretching. This measure, known as the *largest finite-time Lyapunov exponent*, is however not perfect as it incorporates both stretching and shear. As noted by Lapeyre *et al.* (2001), the singular value of X becomes a poor measure of stretching when shear or solid body rotation is too large. Finding an exact quantification of stretching in a given deformation tensor is an active area of research.

Until a more efficient stretching indicator is developed, we use the Lyapunov exponent to approximate stretching and compute LCSs. As shown in figure 7, all the LCSs shown in §3 were computed using this simple method. Thin lines of extremely high stretching are clearly visible and correspond to LCSs. At first, one may be baffled by such plots where clear sharp LCSs become dim in some areas (see, for example, the tip of the lobes in figure 7). The results of Shadden *et al.* (2005) showed, however, that one should not seek lines of maximum stretching. Instead, the LCS is characterized by stretching that drops rapidly in the normal direction. The absolute value of the Lyapunov exponent is usually large along the LCS, but the theory allows for significantly smaller stretching too. What matters is the sharp lateral drop along the LCS, not the absolute value of the exponent.

To get an idea of what an LCS is, it is useful to see the Lyapunov exponent as an altitude field. In other words, one can view the colour map in figure 7 as a topographic map where red denotes high altitude and blue the bottom of deep valleys. The LCS corresponds to a *ridge* or a continental divide in this landscape. If a walker follows a ridge, his on her fate is uncertain in the case of a fall. Depending on the initial impulsion, the unfortunate walker may fall on either side of the ridge. The notion of ridge is an essential ingredient in the definition of the LCS and it connects with the dynamical properties of the LCS: they are lines

dividing regions of different dynamics (valleys) and, as a result, they are 'hotspots' where small perturbations can push particles into different valleys (anticlockwise left cell or clockwise right cell).

5. Surface transport in Monterey Bay

(a) A radar array in Monterey Bay

The concepts of the strongest hyperbolic trajectories and LCSs are not only elegant and exciting mathematical concepts but also robust tools that can be applied easily to many problems in continuous mechanics. To illustrate this aspect, we consider a coastal current observation system in Monterey Bay along the California coastline. The bay is equipped with an array of high-frequency (HF) radar antennas that are able to determine the net displacement of surface particles during 1 h time intervals (Paduan & Rosenfeld 1996). Every hour, the radar data are averaged in circles of radii 3 km and mapped onto a 1 km$\times$1 km grid. The radar data are used directly to approximate the surface trajectories $\boldsymbol{x}(t;\, t_0,\, \boldsymbol{x}_0)$ and permits the computation of LCSs in real time, based on measured ocean conditions.

We begin our study with modal analysis of the HF radar data (Lekien *et al.* 2004). It is, indeed, important to check the energy spectrum and determine whether the flow regime is laminar, quasi-turbulent or turbulent. Haynes (2003) showed that, if the velocity gradient is larger at small scales than at large scales, then there may be patchy stretching areas (subject to turbulent mixing), rather than organized coherent structures. After verifying these hypotheses, we present the LCSs in Monterey Bay and describe the dynamics during an upwelling event. Two applications of LCSs in the bay are presented: the optimal deployment of drifting sensors and the control of the impact of a pollution source.

(b) Energy spectrum in Monterey Bay

There are flows where turbulent diffusion dominates and LCSs are irrelevant. We must determine whether the surface currents of Monterey Bay are laminar, turbulent or quasi-turbulent. Lekien *et al.* (2004) derived a modified Fourier transform that provides the energy spectrum (i.e. the kinetic energy per unit of wavenumber) as a function of the wavenumber ($k{=}2\pi/l$, where l is the length scale).

In a laminar flow, the energy is confined to a small range of length scales. Figure 8 shows that the flow in Monterey Bay is not laminar; there is a significant amount of energy at small length scales (i.e. at large k). Is it turbulent or quasi-turbulent? Most theories on fully established turbulence require that the energy drops slowly enough. This translates into energy spectra behaving as $k^{-5/3}$ or k^{-1}. In Monterey Bay, however, the energy spectrum evolves as k^{-3} (figure 8), a much steeper slope that is commonly observed in quasi-turbulence (Ishihara & Kaneda 2001; Tung & Orlando 2003). Owing to the averaging in the radar installation, the signal vanishes rapidly after the 6 km wavelength. Below 3 km (the radius of the averaging circle), we cannot determine the kinetic energy. It should be clear that there is still a significant portion of the energy in length scales shorter than 3 km, and that improvements in sensing technologies will gradually give us more complete spectra.

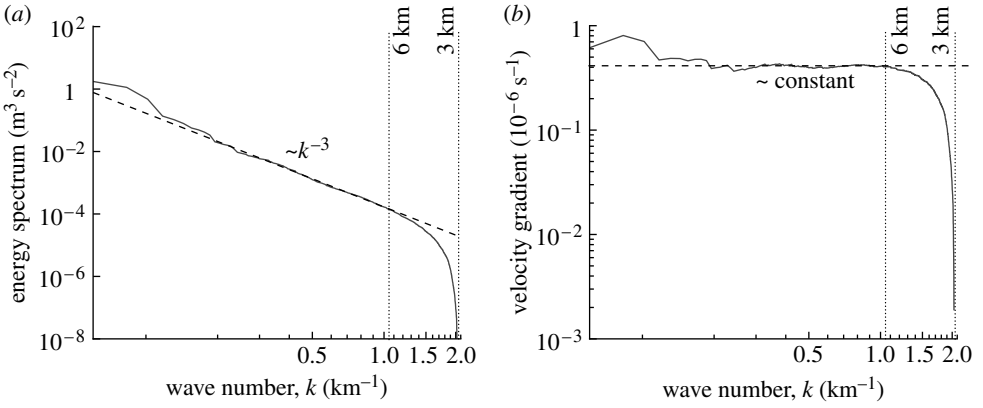

Figure 8. (*a*) Energy spectrum and (*b*) velocity gradient as a function of $k=2\pi/l$.

Defining a boundary between the quasi-turbulent and turbulent regimes is still the topic of many debates but, in the context of the relative importance of stirring and mixing, the velocity gradient gives us a rather clear demarcation line. Recall that the velocity gradient is responsible for the stretching of fluid elements. If the velocity gradient is high only at large scales, it takes a long time to obtain thin filaments of fluid that can be diffused. These flows are dominated by chaotic stirring and correspond to energy spectra $k^{-\gamma}$ where $\gamma \geq 3$. At the limit k^{-3}, the velocity gradient is constant at all length scales. Figure 8 shows that this is indeed the case for Monterey Bay. We conclude that Monterey Bay is a quasi-turbulent flow where particle dynamics are governed by large-scale LCSs, but it is also a complex flow that has features at all length scales and time scales.

Note that we would still be able to apply the LCSs theory if the energy spectrum was decreasing more slowly than k^{-3}. In this case, however, chances are that the dynamics would not be governed by large-scale LCSs. Furthermore, turbulent mixing may overpower chaotic stirring and LCSs. For example, a $k^{-5/3}$ spectrum induces a velocity gradient that evolves as $k^{2/3}$. In such a turbulent flow, the velocity gradient is so high at the Kolmogorov length scale that diffusion is immediate and chaotic stirring irrelevant (Haynes 2003). The case of Monterey Bay is therefore an excellent test bed of the LCS theory: the flow is not fully turbulent, but it has a broad energy spectrum requiring an aperiodic LCS theory.

(*c*) *Dynamics in Monterey Bay*

As shown in figure 9*a* and in Lekien & Haller (in press), the dynamics of particles at the surface of Monterey Bay in August 2003 is governed by a moving repulsive LCS that attaches to the Monterey Peninsula. The LCS divides the domain into two regions of qualitatively different dynamics: recirculation inside a lobe of the LCS and quick escape to the Pacific Ocean on the other side of the LCS.

During the summer months, the bay oscillates regularly between the upwelling events (cold, salty water surfacing and strong southward jet) and relaxation events (weaker, less organized currents and often narrow northward band). The LCS shown in figure 9 is typical of the upwelling regime. It exists

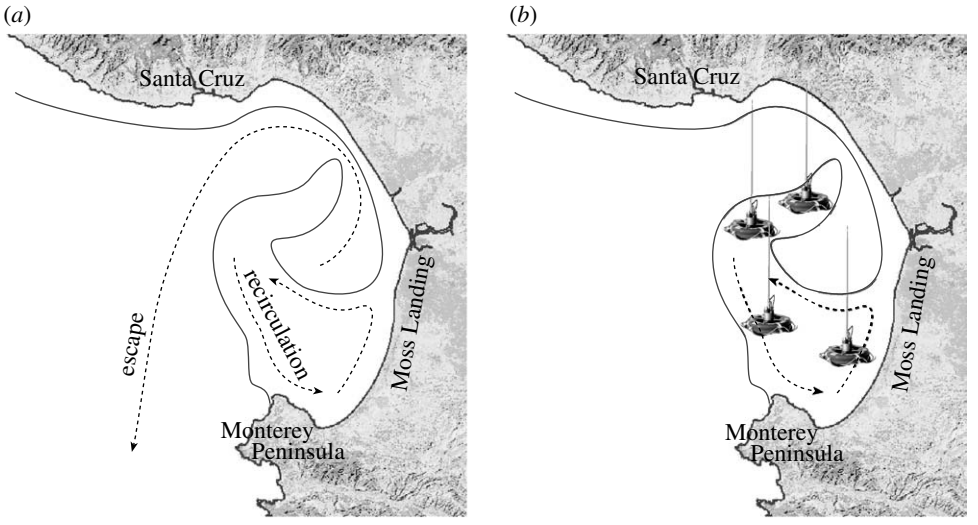

Figure 9. Surface dynamics in Monterey Bay (12.00 GMT on 10 August 2006). A moving LCS (solid line) separates a recirculation zone from a quick clearance alleyway. To keep drifting buoys inside the bay, deployment is concentrated inside the main loop of the LCS.

only for a 3–5 day period after which it is replaced by relaxation LCSs. Note that the radar array captures only the surface dynamics. Strong divergence in the data indicates that there is also a significant motion in the vertical direction during upwelling events (Paduan & Rosenfeld 1996). The availability of acoustic current profiler data at lower depths and recent theoretical developments (Lekien *et al.* 2007) will eventually permit the computation of three-dimensional LCSs in Monterey Bay. In the present paper, however, we concentrate on surface dynamics. This setting is therefore appropriate for studying drifters and floating contaminants. In particular, the divergence in the surface flow is not filtered out and the tracers properly accumulate in the regions with negative divergence.

It is also worth noting that there is an attractive LCS that shoots off Santa Cruz during the upwelling regime. The two LCSs may or may not intersect but, if they intersect, the resulting lobes are rarely observed as the lifetime of the structures is often shorter than the advection time of the lobes. Nevertheless, the repulsive LCS shown in figure 9 provides enough information about surface particle transport and sensitivity to initial conditions for most applications.

Clearly the radar data are not perfect: there are poor and missing data points. To compute LCS from the observed currents, several options are available. First, one can ignore the gaps and assimilate them as immobile particles. Second, one can use the nearest or natural neighbours interpolation (Sibson 1981). It is also possible to fill the gaps and filter spurious data points using optimal interpolation (Gandin 1963) or open-boundary modal analysis (Lekien *et al.* 2004). The LCSs shown in figure 9 are obtained by filling the gaps with immobile particles. Luckily, all these methods produce similar LCSs. This robustness was investigated by Haller (2002) and corroborated by recent studies. Lermusiaux *et al.* (2006) verified the existence of the LCS in figure 9

using the Harvard Ocean Prediction System. Later, Shadden *et al.* (in press) showed that paths of ocean drifters and LCSs in the radar data are in remarkable agreement.

The robust dynamical framework delineated by the LCSs can be exploited for various transport problems and we describe two of them: the deployment of drifting sensors and coastal pollution mitigation.

(*d*) *Application: optimal drifter deployment*

Monterey Bay is regularly the site of large-scale scientific experiments during which scientists from various fields deploy and use aircraft, boats, underwater vehicles, buoys and ocean models. Leonard *et al.* (2007) described field experiments in Monterey Bay and highlight the importance of coordinating the assets in such a way that they collect the maximum information. Indeed, two buoys which are too close to each other measure data that are strongly correlated and act almost as a single sensor. Leonard *et al.* (2007) also emphasized the importance of using large arrays of cheap vehicles. Among those weaker vehicles, we find underwater gliders and drifters. While typical propelled underwater vehicles run only for a few hours and must be constantly recovered and launched from a boat, underwater gliders use a buoyancy engine and stay at sea for several weeks or months. This autonomy comes at the expense of power: gliders move slowly, cannot always fight the strong currents in the bay and must be operated carefully in order to profit from ocean dynamics. As described by Bhatta *et al.* (2005), LCSs in Monterey Bay provide a visual description of the flow and can assist in designing optimal control of groups of gliders.

Figure 9*b* illustrates the use of LCS for deploying drifting buoys. In this case, the sensors are not actuated at all. From the initial configuration, each drifter follows the currents. Based on our analysis of the dynamics in the bay, these drifters will typically have two types of behaviour: they either recirculate in the bay or go out into the open ocean. During an experiment, vehicles should remain inside the domain as much as possible. Indeed, when a drifter goes off into the Pacific Ocean, one must either send a boat to pick it up or abandon the asset. Both options are costly and waste available resources. Therefore, the initial deployment of drifters requires careful planning in order to identify the optimal strategy. As shown in figure 9*b*, the drifters are concentrated inside the lobe of the LCS, which guarantees that they will recirculate in the bay (Shadden *et al.* in press).

(*e*) *Application: optimal coastal discharge*

Monterey Bay is a natural preserve confronted with several sources of pollution. Two of them are located in the Moss Landing area: the Elkhorn Slough and the Duke Energy power plant. In particular, warm water is expelled from the power plant through a 600 m pipe (Coulliette *et al.* in press).

In figure 10, a pipe is represented and we follow the evolution of released pollutants. Depending on the position of the LCS, the behaviour of the pollutants may vary to a considerable degree. At 12.00 GMT on 10 August (figure 10*a*), the end of the pipe falls inside the loop of the LCS, and the pollutants will recirculate in the bay. This large amount of pollutants in a shallow area induces peaks of

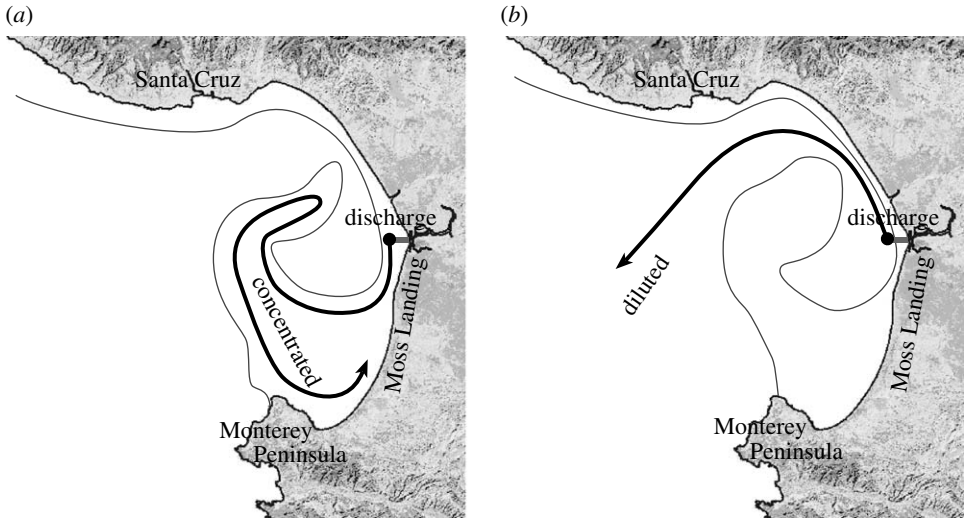

Figure 10. Optimal timing for the release of coastal pollutant. If pollutants are discharged in the bay, their outcome varies, depending on the position of the LCS with respect to the pipe outlet. (*a*) 12.00 GMT on 10 August 2006. (*b*) 18.00 GMT on 10 August 2006.

pollution and devastates the environment. The LCS is, however, mobile and, 6 h later, it moved east of the pipe outlet (figure 10*b*). In this case, pollutants are no longer released into the recirculation zone, but are quickly advected towards the ocean. These pollutants mix with a large quantity of water and their impact on the ecosystem is much less dramatic.

Smith (1998) suggested using holding tanks to reduce the impact of pollutants. A source of pollution is virtually interrupted by diverting pollutants to the tank. The tank can be emptied later when the pollutants will have a lesser impact. Using LCS and, in particular, the position of the LCS with respect to the pipe outlet, we are able to identify periods of recirculation (i.e. when the pollutants must be diverted to the holding tank) and periods of quick clearance (i.e. when the tank is emptied and the pollution released). Coulliette *et al.* (in press) showed how such a combination of holding tanks and LCS monitoring can *reduce the impact of coastal discharge while not changing the total amount of released pollutants*.

This concept of 'intelligent coastal discharge' is becoming increasingly appealing in the light of the many environmental threats faced by the planet. Feeding the growing human population cannot be achieved without a minimal pollution. At best, human activity will still generate thermal pollution. Once a minimal discharge is achieved, understanding contaminant dynamics and fate becomes our only option for minimizing environmental damages.

6. Conclusion

Chaotic stirring and turbulent mixing used to be studied separately in laminar and turbulent flows, respectively. Most flows in nature are, however, found in an intermediate regime. The discovery of these quasi-turbulent flows called for a better understanding of the interaction of advection and diffusion.

The nascent LCS theory aims at understanding chaotic stirring in these flows. Its efficiency stems from its ability to deal with large velocity gradients at all scales, and its robustness with respect to velocity fluctuations and uncertainties. As a result, it can already be used in conjunction with ocean sensing networks to optimize the deployment of buoys or for coastal pollution mitigation.

To pursue our understanding of chaotic stirring in quasi-turbulent flows, LCS theory must, however, still address the following three fundamental issues.

— *The ambiguity between the notion of finite-time invariant and quasi-invariant manifolds.* Defining LCS using invariant manifolds gives a paradigm that is closer to the transport properties of steady and periodic systems, as well as the Smale horseshoe. Unfortunately, this also precludes bifurcations of the LCSs. When LCSs are defined as ridges of a stretching indicator, such as the Lyapunov exponent, they become almost invariant. These LCSs can bifurcate and change according to seasonal variations in the flow dynamics. Physically, the latter approach is more able to describe transport in aperiodic fluids that oscillate between various regimes, such as upwelling and relaxation in Monterey Bay. Mathematically, the notion of quasi-invariant manifold is not well developed and LCSs suffer from this lack of formalism.
— *The quantification of stretching in the finite deformation tensor* to overcome the deficiencies of the Lyapunov exponent.
— *A deeper understanding of the subtle interaction between stirring and mixing.* The LCSs, which govern chaotic stirring, are lines of maximum stretching and, as a result, are also zones where mixing is important. A global spectral analysis alone cannot explain the subtle interaction between stirring and mixing and local investigations of tracer transport near the LCSs are needed.

We are grateful to Peter Haynes (University of Cambridge) and Jacques Vanneste (University of Edinburgh) for enlightening discussions. Some sections of this paper were strongly influenced by the talks of Peter Haynes and Jacques Vanneste at the Tropical Scalar Transport Meeting of the National University of Singapore. This research also profited from the help and comments of George Haller (Massachusets Institute of Technology), Naomi Leonard (Princeton University), Jerry Marsden (California Institute of Technology), Raphaël Robiette (Université Catholique de Louvain), Goldie Scarr-Blankoff (Institut Supérieur de Traducteurs et Interprètes) and Shawn Shadden (Stanford University).

References

Arfken, G. 1985 *Mathematical methods for physicists*, 3rd edn. Orlando, FL: Cambridge University Press.

Bhatta, P. *et al.* 2005 Coordination of an underwater fleet for adaptive sampling. In *Int. Workshop on Underwater Robotics*, pp. 61–69.

Cellier, F. E. & Kofman, E. 2006 *Continuous system simulation.* Secaucus, NJ: Springer.

Coulliette, C. & Wiggins, S. 2001 Intergyre transport in a wind-driven, quasigeostrophic double gyre: an application of lobe dynamics. *Nonlin. Process. Geophys.* **8**, 69–94.

Coulliette, C., Lekien, F., Haller, G., Paduan, J. & Marsden, J. E. In press. Optimal pollution mitigation in Monterey Bay based on coastal radar data and nonlinear dynamics. *Environ. Sci. Technol.*

Gandin, L. S. 1963 *Gidrometerologicheskoe izdatelstvo-objective analysis of meteorological fields.* [English transl. Israeli Program for Scientific Translations, Leningrad, Jerusalem.] Leningrad, Russia; Jerusalem, Israel: Israeli Program for Scientific Translations.

Giona, M., Cerbelli, S. & Adrover, A. 2002 Quantitative analysis of mixing structures in chaotic flows generated by infinitely fast reactions in the presence of diffusion. *J. Phys. Chem. A* **106**, 5722–5736. (doi:10.1021/jp013781e)

Guckenheimer, J. & Holmes, P. J. 1983 *Nonlinear oscillations, dynamical systems, and bifurcations of vector fields*. New York, NY; Berlin, Germany: Springer.

Haller, G. 2000 Finding finite-time invariant manifolds in two-dimensional velocity fields. *Chaos* **10**, 99–108. (doi:10.1063/1.166479)

Haller, G. 2002 Lagrangian coherent structures from approximate velocity data. *Phys. Fluids A* **14**, 1851–1861. (doi:10.1063/1.1477449)

Haller, G. & Poje, A. C. 1998 Finite-time transport in aperiodic flows. *Physica D* **119**, 352–380. (doi:10.1016/S0167-2789(98)00091-8)

Haynes, P. H. 2003 Turbulence and mixing. In *Encyclopedia of the atmospheric sciences*. Amsterdam, The Netherlands: Elsevier.

Hinze, J. O. 1975 *Turbulence*. New York, NY: McGraw-Hill.

Ide, K., Small, D. & Wiggins, S. 2002 Distinguished hyperbolic trajectories in time-dependent fluid flows: analytical and computational approach for velocity fields defined as data sets. *Nonlin. Process. Geophys.* **9**, 237–263.

Ishihara, T. & Kaneda, Y. 2001 Energy spectrum in the enstrophy transfer range of two-dimensional forced turbulence. *Phys. Fluids* **13**, 544–547. (doi:10.1063/1.1336149)

Koh, T.-Y. & Legras, B. 2002 Hyperbolic lines and the stratospheric polar vortex. *Chaos* **12**, 382–394. (doi:10.1063/1.1480442)

Kolmogorov, A. N. 1941 Local structure of turbulence in an incompressible viscous fluid at very high reynolds numbers. *Dokl. Akad. Nauk. SSSR* **30**, 299.

Lapeyre, G., Hua, B. L. & Legras, B. 2001 Comments on "finding finite-time invariant manifolds in two-dimensional velocity fields" [*Chaos* **10**, 99 (2000)]. *Chaos* **11**, 427–430. (doi:10.1063/1.1374241)

Lekien, F. & Haller, G. In press. Unsteady flow separation on slip boundaries. *Phys. Fluids*.

Lekien, F. & Leonard, N. E. 2004 Dynamically consistent Lagrangian coherent structures. In *Experimental chaos*, vol. 742, pp. 132–139. Washington, DC: American Institute of Physics.

Lekien, F., Coulliette, C., Bank, R. & Marsden, J. E. 2004 Open-boundary modal analysis: interpolation, extrapolation, and filtering. *J. Geophys. Res.* **109**, C12004. (doi:10.1029/2004JC002323)

Lekien, F., Shadden, S. C. & Marsden, J. E. 2007 Lagrangian coherent structures in n-dimensional systems. *J. Math. Phys.* **48**, 065404. (doi:10.1063/1.2740025)

Leonard, N. E., Paley, D. A., Lekien, F., Sepulchre, R., Fratantoni, D. M. & Davis, R. E. 2007 Collective motion, sensor networks, and ocean sampling. *Proc. IEEE* **95**, 48–74. (doi:10.1109/JPROC.2006.887295)

Lermusiaux, P. F. J. *et al.* 2006 Quantifying uncertainties in ocean predictions. *Oceanography* **19**, 90–103.

Lorenz, E. N. 1963 Deterministic nonperiodic flow. *J. Atmos. Sci.* **20**, 130–141. (doi:10.1175/1520-0469(1963)020<0130:DNF>2.0.CO;2)

Mancho, A., Small, D. & Wiggins, S. 2004 Computation of hyperbolic trajectories and their stable and unstable manifolds for oceanographic flows represented as data sets. *Nonlin. Process. Geophys.* **11**, 17–33.

Olascoaga, M. J., Rypina, I. I., Brown, M. G., Beron-Vera, F. J., Kocak, H., Brand, L. E., Halliwell, G. R. & Shay, L. K. 2006 Persistent transport barrier on the West Florida shelf. *Geophys. Res. Lett.* **33**, L22603. (doi:10.1029/2006GL027800)

Ottino, J. M. 1990 Mixing, chaotic advection, and turbulence. *Annu. Rev. Fluid Mech.* **22**, 207–253. (doi:10.1146/annurev.fl.22.010190.001231)

Paduan, J. D. & Rosenfeld, L. K. 1996 Remotely sensed surface currents in Monterey Bay from shore-based HF radar (coastal ocean dynamics application radar). *J. Geophys. Res. Oceans* **101**, 20 669–20 686. (doi:10.1029/96JC01663)

Parker, T. S. & Chua, L. O. 1989 *Practical numerical algorithm for chaotic systems*, 3rd edn. New York, NY: Springer.

Poincaré, H. 1890 *Les Méthodes Nouvelles de la Mécanique Céleste*. Paris, France: Gauthier-Villars.

Poje, A. C. & Haller, G. 1999 Geometry of cross-stream mixing in a double-gyre ocean model. *J. Phys. Oceanogr.* **29**, 1649–1665. (doi:10.1175/1520-0485(1999)029<1649:GOCSMI>2.0.CO;2)

Rom-Kedar, V. 1990 Transport rates of a class of two-dimensional maps and flows. *Physica D* **43**, 229–268. (doi:10.1016/0167-2789(90)90135-C)

Rom-Kedar, V. & Poje, A. C. 1999 Universal properties of chaotic transport in the presence of diffusion. *Phys. Fluids* **11**, 2044–2057. (doi:10.1063/1.870067)

Ross, S. D. 2006 The interplanetary transport network. *Am. Sci.* **94**, 230. (doi:10.1511/2006.3.230)

Sandstede, B., Balasuriya, S., Jones, C. K. R. T. & Miller, P. 2000 Melnikov theory for finite-time vector fields. *Nonlinearity* **13**, 1357–1377. (doi:10.1088/0951-7715/13/4/321)

Shadden, S. C., Lekien, F. & Marsden, J. E. 2005 Definition and properties of Lagrangian coherent structures from finite-time Lyapunov exponents in two-dimensional aperiodic flows. *Physica D* **212**, 271–304. (doi:10.1016/j.physd.2005.10.007)

Shadden, S. C., Lekien, F., Paduan, J. D., Chavez, F. & Marsden, J. E. In press. The correlation between surface drifters and coherent structures based on high-frequency radar data in Monterey Bay. *Deep Sea Res.*

Sibson, R. 1981 A brief description of natural neighbor interpolation. In *Interpreting multivariate data*, pp. 21–36. Chichester, UK: Wiley.

Smale, S. 1980 *The mathematics of time: essays on dynamical systems, economic processes, and related topics*. New York, NY; Berlin, Germany: Springer.

Smith, R. 1998 Using small holding tanks to reduce pollution in narrow estuaries. *J. Hydraulic Eng.* **124**, 117–122. (doi:10.1061/(ASCE)0733-9429(1998)124:2(117))

Solomon, T. H. & Gollub, J. P. 1988 Passive transport in steady Rayleigh–Bénard convection. *Phys. Fluids* **31**, 1372–1379. (doi:10.1063/1.866729)

Stewart, I. 1989 *Does god play dice? The mathematics of chaos*. London, UK: Penguin Books.

Tél, T., De Moura, A., Grebogi, C. & Károlyi, G. 2005 Chemical and biological activity in open flows: a dynamical system approach. *Phys. Rep.* **413**, 91–196. (doi:10.1016/j.physrep.2005.01.005)

Tung, K. K. & Orlando, W. W. 2003 The k^{-3} and $k^{-5/3}$ energy spectrum of atmospheric turbulence: quasigeostrophic two-level model simulation. *J. Atmos. Sci.* **60**, 824–835. (doi:10.1175/1520-0469(2003)060<0824:TKAKES>2.0.CO;2)

Varotsos, C. 2002 The Southern Hemisphere ozone hole split in 2002. *Environ. Sci. Pollut. Res.* **9**, 375–376.

Voth, G. A., Haller, G. & Gollub, J. P. 2002 Experimental measurements of stretching fields in fluid mixing. *Phys. Rev. Lett.* **88**, 254501,1-4. (doi:10.1103/physRevLett.88.254501)

AUTHOR PROFILES

Francois Lekien (left)

Francois Lekien was born in Brussels, Belgium in 1976. He graduated from the École Polytechnique of the Université Libre de Bruxelles in 1999 and received a PhD in control and dynamical systems from the California Institute of Technology in 2003.

Francois was a postdoctoral scholar in mechanical engineering at the Massachusets Institute of Technology, and then a research associate in mechanical and aerospace engineering at Princeton University. He is now a professor of applied mathematics at the Université Libre de Bruxelles.

His interests include nonlinear dynamics in quasi-turbulent flows, coherent structures and modal reconstruction of coastal currents.

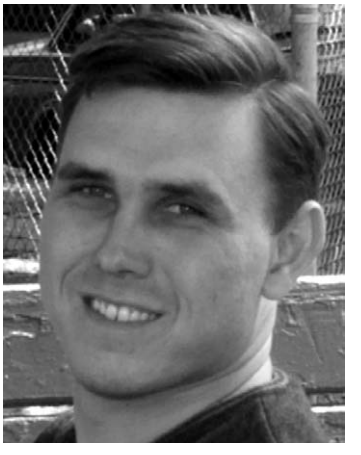

Chad Coulliette (right)

Chad Coulliette received a BS degree in mechanical engineering and MS degree in aerospace engineering from the Northern Arizona University in 1992 and 1994, respectively. He received MS and PhD degrees in chemical engineering from the University of California, San Diego in 1995 and 1996, respectively.

In 1997, Chad joined the department of control and dynamical systems at the California Institute of Technology and began investigating on chaotic transport in Monterey Bay.

In 2003, Chad began suffering serious complications from a spinal cord injury. He is now working from his family home in Mesa, Arizona. Chad concentrates his efforts on understanding coherent structures and chaotic dynamics in fluids and on applying these concepts to environmental problems.